Since January 2020 Elsevier has created a COVID-19 resource centre with free information in English and Mandarin on the novel coronavirus COVID-19. The COVID-19 resource centre is hosted on Elsevier Connect, the company's public news and information website.

Available online at www.sciencedirect.com
SCIENCE DIRECT
Virus Research 114 (2005) 70–79
Virus Research
www.elsevier.com/locate/virusres

Nucleolar localization of non-structural protein 3b, a protein specifically encoded by the severe acute respiratory syndrome coronavirus

Xiaoling Yuan [1], Zhenyu Yao [1], Yajun Shan, Bo Chen, Zhen Yang, Jie Wu, Zhenhu Zhao, Jiapei Chen, Yuwen Cong *

Department of Pathophysiology, Beijing Institute of Radiation Medicine, No. 27 Taiping Road, Beijing 100850, China

Received 21 February 2005; received in revised form 1 June 2005; accepted 6 June 2005
Available online 25 July 2005

Abstract

The open reading frame 3 (ORF3) of the severe acute respiratory syndrome coronavirus (SARS-CoV) genome encodes a predicted 154-amino acid protein, which lacks similarities to any known protein, and is named 3b. In this study, it was shown that 3b protein was predominately localized to nucleus with EGFP tag at its N- or C-terminus. The localization patterns were similar in different transfected cells. Immunofluorescence assay revealed that 3b protein was co-localized well with C23 in nucleolus. C23, B23 and fibrillarin all are important nucleolar proteins, which localize in the region of the nucleolus. Co-transfection of p3b-EGFP with pC23-DsRed, pB23-DsRed and pfibrillarin-DsRed further confirmed 3b's nucleolus localization. With construction of serial truncated mutants of 3b, a region (residues 134–154 aa) responsible for nucleolar localization was determined in 3b protein. These results provide a new insight for further functional studies of SARS-CoV 3b protein.

1. Introduction

The outbreak of severe acute respiratory syndrome (SARS), which originated in early November 2002, in the Guangdong province of People's Republic of China, posed a great global threat. A total of 8422 cases have been reported to World Health Organization from 32 countries or special regions with 916 related deaths reported (Fan et al., 2004; Lee et al., 2003; Peiris et al., 2003; Tsang et al., 2003; WHO, 2003). SARS is a system disease that impairs many organs, such as lung, liver and immune organs. Respiratory distress and decreased immune function are proposed to be the main causes of SARS patient death (Ding et al., 2003; Lang et al., 2003; Nicholls et al., 2003). Under the leading and coordination by the WHO, SARS was found to be caused by a novel coronavirus, which was designated as SARS coronavirus (SARS-CoV). The complete sequence of SARS-CoV genome was then determined by several research groups (Drosten et al., 2003; Fouchier et al., 2003; Ksiazek et al., 2003; WHO, 2003). It was revealed that the genome of SARS-CoV contains 11 to 14 open reading frames (ORF), which encode replicase 1A, replicase 1B, four structure proteins (spike, S; envelope, E; membrane, M; nucleocapsid, N) and five to eight potential non-structural proteins (Marra et al., 2003; Rota et al., 2003). Published data proposed that coronavirus accessory proteins, varying in size and position in the genome of coronaviruses, might be dispensable for virus replication, at least in the cell culture system, but may be important for virus–host interaction (Haijema et al., 2004). For example, mutants or deletion of one of these proteins, such as 7b gene of feline coronavirus or gene 3 of swine enteric and respiratory coronavirus, have been reported to be related to the reduced virulence and pathogenesis (Herrewegh et al., 1995; Paul et al., 1997).

Abbreviations: DMEM, Dulbecco's modified Eagel's medium; ECL, enhanced chemiluminescence; EGFP, enhanced green fluorescent protein; N, nucleocapsid; NLS, nuclear localization signal; NoLS, nucleolus localization signal; ORF, open reading frame; PBS, phosphate-buffered saline; SARS, severe acute respiratory syndrome; SARS-CoV, SARS coronavirus

* Corresponding author. Tel.: +86 10 66931223; fax: +86 10 68214653.
E-mail address: congyw@nic.bmi.ac.cn (Y. Cong).

[1] These authors contributed equally.

0168-1702/$ – see front matter © 2005 Elsevier B.V. All rights reserved.
doi:10.1016/j.virusres.2005.06.001

The ORF of SARS-CoV X2, named 3b by Thiel, encodes 154 amino acids (CDS: 25680-26144), overlapping entirely with ORF3a and E protein, and may be expressed from the ORF3 using an internal ribosomal entry site (Rota et al., 2003; Thiel et al., 2003). Bioinformatics analysis showed that SARS-CoV 3b protein did not match any known sequences as well as 3b protein of other coronavirus members (Marra et al., 2003). The ORF3 in the known coronavirus has been demonstrated to be functionally bicistronic or tricistronic, which coded 3a, 3b and 3c (for E) protein (Le et al., 1994; Liu and Inglis, 1992). Published studies revealed that ORF3b was expressed in coronavirus infectious bronchitis virus (IBV) and porcine transmissible gastroenteritis (TGEV) infected cells (Curtis et al., 2002; Liu et al., 1991; Shen et al., 2003). It was further reported that 3b protein of IBV was localized in the nucleus and took part in the pathogenesis and replication of IBV (Shen et al., 2003). Till now, there is no report on SARS-CoV 3b protein. In this study, we present data demonstrating that (i) 3b protein was capable of localizing to nucleus in the absence of any additional viral proteins, (ii) 3b protein was co-localized with nucleolus marker proteins C23/nucleolin, B23/nucleophosmin and fibrillarin in transfected cells, (iii) and the regions required for nucleolar localization were identified.

2. Materials and methods

2.1. Cell culture and transfection

293 (human embryonic kidney fibroblast) cells, Vero (African green monkey kidney epithelial) cells and COS-7 (African green monkey kidney fibroblast) cells were grown in Dulbecco's modified Eagel medium (DMEM) (Gibco BRL) supplemented with 10% FBS. A549 (human lung carcinoma) cells were cultured in Ham's F12K medium with 10% FBS at 37 °C in a incubator supplied with 5% CO_2. When cell density in a culture plate reached 70% confluence, cells were transfected with 1.5 μg/ml plasmid DNA using Lipofectamine™ 2000 (Invitrogen) according to manufacturers' instruction. The medium was replaced with fresh medium 5 h after transfection and then incubated until experiment.

2.2. Construction of p3b-EGFP, pEGFP-3b, serial of truncated 3b protein and pC23-DsRed, pB23-DsRed, pfibrillarin-DsRed

The 3b used for this study was PCR amplified from SARS-CoV (ZJ01, AY297028) genome by using Taq DNA polymerase (NEB). PCR was performed with a forward primer (containing an *Xho*I site) and a reverse primer (containing an *Eco*RI site) complementary to the 3′ end of 3b without stop codon to allow for reading-through. This product was cut with *Xho*I and *Eco*RI, and the obtained gene was cloned into multiple cloning site (MCS) of pEGFP-N1 vector (Clontech), producing a p3b-EGFP plasmid. The pEGFP-3b, truncated 3b constructs were made in a similar fashion, and the oligonucleotide primers used were listed in Table 1. The C23, B23 and fibrillarin genes were PCR amplified from COS-7 cells genome and cloned into pDsRed-N1 vector separately. All plasmid sequences were confirmed by sequencing analysis.

2.3. Expression of p3b-EGFP and pEGFP-3b

The transfected cells were harvested at 48 h after transfection. Total cell lysates preparation and Western blot analysis were performed according to the procedure described before (Yuan et al., 2004). In brief, the cell lysates were prepared, ran on SDS-PAGE, and transferred to PVDF membrane. The membrane was blocked with 5% non-fat milk in TBST (20 mM Tris pH7.5, 150 mM NaCl and 0.05% Tween20), and incubated with monoclonal anti-GFP antibody (1:10,000) (Sigma). Membranes were washed with TBS buffer and incubated with corresponding secondary antibody (Santa Cruz) tagged with horseradish peroxidase for 1 h. Proteins were visualized with enhanced chemiluminescence (ECL) reagents (Cell Signaling Inc.).

2.4. Confocal microscopy analysis

Cellular localization of SARS-CoV 3b protein was prepared according to the procedure described before (Yuan et al., 2005). At 24 h after transfection with p3b-EGFP or co-transfection with pC23-DsRed, pB23-DsRed or pfibrillarin-DsRed, cells on glass cover slips were incubated with actinomycin D (Sigma) at 10 μg/ml for 3 h. Then the cells were rinsed with phosphate buffered saline (PBS), subjected to fixation using 3.7% paraformaldehyde for 30 min and permeabilized with 0.2% Triton X-100. For immune-fluorescence assays, the permeabilized cells were incubated in order with anti-C23 antibody (1:1000) and TRITC-tagged secondary antibody (1:1000, Santa Cruz) for 1 h. Then the nuclei were stained with Hoechst 33342 (0.1 μg/ml) (Molecular Probes) or PI (50 μg/ml) (Sigma). Specimens were examined by confocal fluorescent microscope on a Bio-Rad Radiance 2100 System.

2.5. Prediction of nuclear localization signal (NLS) and hydrophilicity profile

SARS-CoV 3b protein sequences were run through PSORT II server (http://psort.nibb.ac.jp), and NLS was predicted as preset definitions (Nakai and Kanehisa, 1992). In brief, NLS was classified as follows. Classical NLS enriches in basic amino acids and generally conforms to one of three motifs: (1) four-residue pattern (pat4) consists of a continuous residue of three or four basic amino acids (K or R) associated with histidine or proline; (2) seven-residue pattern (pat7) starts with proline and followed by three basic residues out of four; (3) another type of NLS (bipartite) consists of two basic residues, a 10-residue spacer and a region containing at least three basic residues of five. And a

Table 1
Primes used for wild type and deletant 3b constructs[a]

Construct name	Polarity	Sequence
p3b-EGFP	Sense[b]	5′-CCGCTCGAGCGCCACCATGGTGCCAACTACTTTGTTTGCTGGCAC-3′
	Anti-sense[c]	5′-CGGAATTCCACGTACCTGTTTCTTCCGAAACG-3′
3b 133-EGFP	Sense	5’-CCGCTCGAGCGCCACCATGGTGCCAACTACTTTGTTTGCTGGCAC-3′
	Anti-sense	5′-CGGAATTCCACAAAGGCACGCTAGTAGTC-3′
3b 100-EGFP	Sense	5′-CCGCTCGAGCGCCACCACCATGGTGCCAACTACTTTGTTTGCTGGCAC-3′
	Anti-sense	5′-CGGAATTCCGTGGGTCTTTAACAAGCTTG-3′
3b 80-EGFP	Sense	5′-CCGCTCGAGCGCCACCATGGTGCCAACTACTTTGTTTGCTGGCAC-3′
	Anti-sense	5′-CGGAATTCCTAGTAATTTGTGTAGACTCAAGCTGGTAG-3′
3b 68-EGFP	Sense	5′-CCGCTCGAGCGCCACCATGGTGCCAACTACTTTGTTTGCTGGCAC-3′
	Anti-sense	5′-CGGAATTCCCGGTGAAATAGCCATGTAC-3′
3b 45-EGFP	Sense	5′-CCGCTCGAGCGCCACCATGGTGCCAACTACTTTGTTTGCTGGCAC-3′
	Anti-sense	5′-CGGAATTCCTTTGGTAGTCTTCTTTGAGTTTTGG-3′
3b D18-EGFP	Sense	5′-CCGCTCGAGGCCACCACCATGGATATAACAGTGTCACAG-3′
	Anti-sense[c]	5′-CGGAATTCCACGTACCTGTTTCTTCCGAAACG-3′
3b D39-EGFP	Sense	5′-CCGCTCGAGGCCACCATGGCAAAGAAGACTACCAAATTG-3′
	Anti-sense[c]	5′-CGGAATTCCACGTACCTGTTTCTTCCGAAACG-3′
3b D45-EGFP	Sense	5′-CCGCTCGAGGCCACCATGGAATTGGTGGTTATTCTGAGGATAGG-3′
	Anti-sense[c]	5′-CGGAATTCCACGTACCTGTTTCTTCCGAAACG-3′
3b D68-EGFP	Sense	5′-CCGCTCGAGGCCACCATGGCGAAGTTTACTACCAGC-3′
	Anti-sense[c]	5′-CGGAATTCCACGTACCTGTTTCTTCCGAAACG-3′
3b D80-EGFP	Sense	5′-CCGCTCGAGGCCACCACCATGGTACTACAGACACTGGTATTGAAAATG-3′
	Anti-sense[c]	5′-CGGAATTCCACGTACCTGTTTCTTCCGAAACG-3′
3b D124-EGFP	Sense	5′-CCGCTCGAGGCCACCCACCATGAGCCGACGACGACTAC-3′
	Anti-sense[c]	5′-CGGAATTCTGTTTCTTCCGAAACG-3′
3b D134-EGFP	Sense	5′-CCCTCGAGGCCACCATGAAGCACAAGAAAGTGAGTAC-3′
	Anti-sense[c]	5′-CGGAATTCCACGTACCTGTTTCTTCCGAAACG-3′
pC23-DsRed	Sense[b]	5′-CCGCTCTCGAGCGCCACCATGGTGAAGCTCGCGAAGGCAGG-3′
	Anti-sense[c]	5′-CGGAATTCTTCAAACTTCGT CTTCTTTCCTTGTGGCTTG-3′
pB23-DsRed	Sense[b]	5′-CCGCTCTCGAGCGCCACCATGGAAGATTCGATGGACATGGAC-3′
	Anti-sense[c]	5′-CGGAATTCAAGAGACTTCCTCCACTGCCA-3′
pFibrillarin-DsRed	Sense[b]	5′-CCGCTCGAGCGCCACCACCATGAAGCCAGGATTCAGTCCCCG-3′
	Anti-sense[c]	5′-CGGAATTCGTTCTTCACCTTGGGGGGTGGC-3′
pEGFP-3b	Sense	5′-CCCTCGAGCGGCCACCACCATG GTGCCAACTACTTTGTTTGCTGGCAC-3′
	Anti-sense[c]	5′-CGGAATTCACTACGTACCTGTTTCTTCCGAAACG-3′

[a] Gene sequences are correspond to SARS-CoV (ZJ01).
[b] Underlined nucleotides represent restriction site and Kozak sequence before start codon (ATG).
[c] Underlined nucleotides represent restriction site and delete the stop codon.

Hopp–Woods hydrophilicity was predicted according to the Hopp and Woods (Hofmann and Hadge, 1987).

3. Results and discussion

3.1. Cellular localization of SARS-CoV 3b protein

Previous studies revealed that SARS-CoV 3b, encoding a 154-amino acid protein, lacks significant similarities to any previously known proteins (Drosten et al., 2003; Marra et al., 2003). Bioinformatics analysis using PSORT II server showed that two potential nuclear localization signals (NLS) were predicted in 3b protein. NLS1, located at aa135–138 (KHKK), comprises pattern 4 sequences, and bipartite NLS, located at aa137–153 (KKVSTNLCTHSFRKKQV), overlaps with pattern 4 sequences. Furthermore, Hopp–Woods hydrophilicity analysis of 3b protein (Hofmann and Hadge, 1987) revealed that the predicted putative NLS was in hydrophililic regions and easily accessible. No signal peptides, coiled-coil regions and transmembrane region allocation were detected. To learn more function about it, the gene of 3b from SARS-CoV genome (ZJ01, AY297028) was cloned into pEGFP-N1 and pEGFP-C1 vectors and expressed in 293 cells (Fig. 1A). Western blot analysis with anti-GFP antibody demonstrated that chimeric proteins was expressed

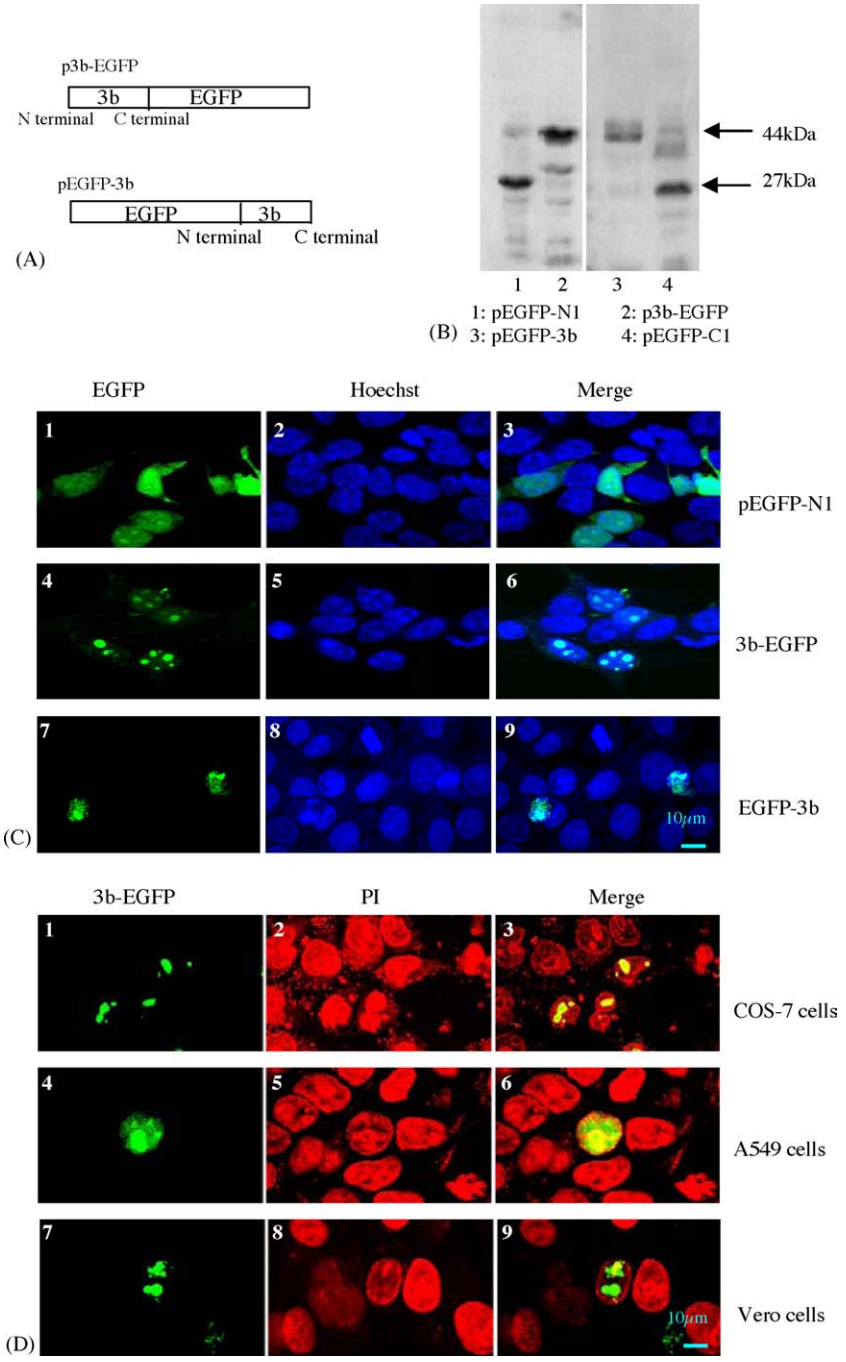

Fig. 1. Expression and cellular localization of 3b in transfected cells. (A) Constructs of p3b-EGFP and pEGFP-3b. The 3b from SARS-CoV genome was cloned as a C-terminal fusion to pEGFP-N1 vector, and as N-terminal fusion to pEGFP-C1 vector. (B) Western blot analysis. 293 cells were transiently transfected with pEGFP-N1, p3b-EGFP, pEGFP-3b and pEGFP-C1 plasmids separately. Cell lysates were prepared at 24 h after transfection and separated by SDS-PAGE. Protein transferred to PVDF membrane was probed with monoclonal anti-GFP antibody. Sizes (kDa) of molecular mass markers were indicated on the right. (C) Cellular localization of 3b protein. 293 cells were transfected with described plasmids separately, cellular localization of 3b was observed by confocal fluorescence microscope. Green represented EGFP fluorescence (1, 4 and 7) from original pEGFP, p3b-EGFP or pEGFP-3b; blue (2, 5 and 8) represented Hoechst 33342 stained cell nuclei; images 3, 6 and 9 represented overlapping of green and blue fluorescence. All three panels of a row have the same field of view. (D) Cellular localization of 3b protein in different cells. COS-7, Vero and A549 cells were transiently transfected with p3b-EGFP separately. Cellular localization of 3b was observed at 24 h after transfection. Green represented EGFP fluorescence from expressed p3b-EGFP in different cells; the overlay image represented green and red (from PI staining nuclei) fluorescence. All three panels of a row have the same field of view.

and migrated at the expected molecular mass of approximately 44 kDa (Fig. 1B).

Next, the cellular localization of 3b protein fused with EGFP at N- or C-terminus was tested by fluorescence confocal microscopy. As shown in Fig. 1C, EGFP protein was distributed diffusely throughout both cytoplasm and nucleus in transfected 293 cells. However, the fluorescence pattern of 3b-EGFP and EGFP-3b was displayed small bright dots within nucleus and some moderate to faint signal in the cytoplasm. It was also found that the EGFP tag at its N-

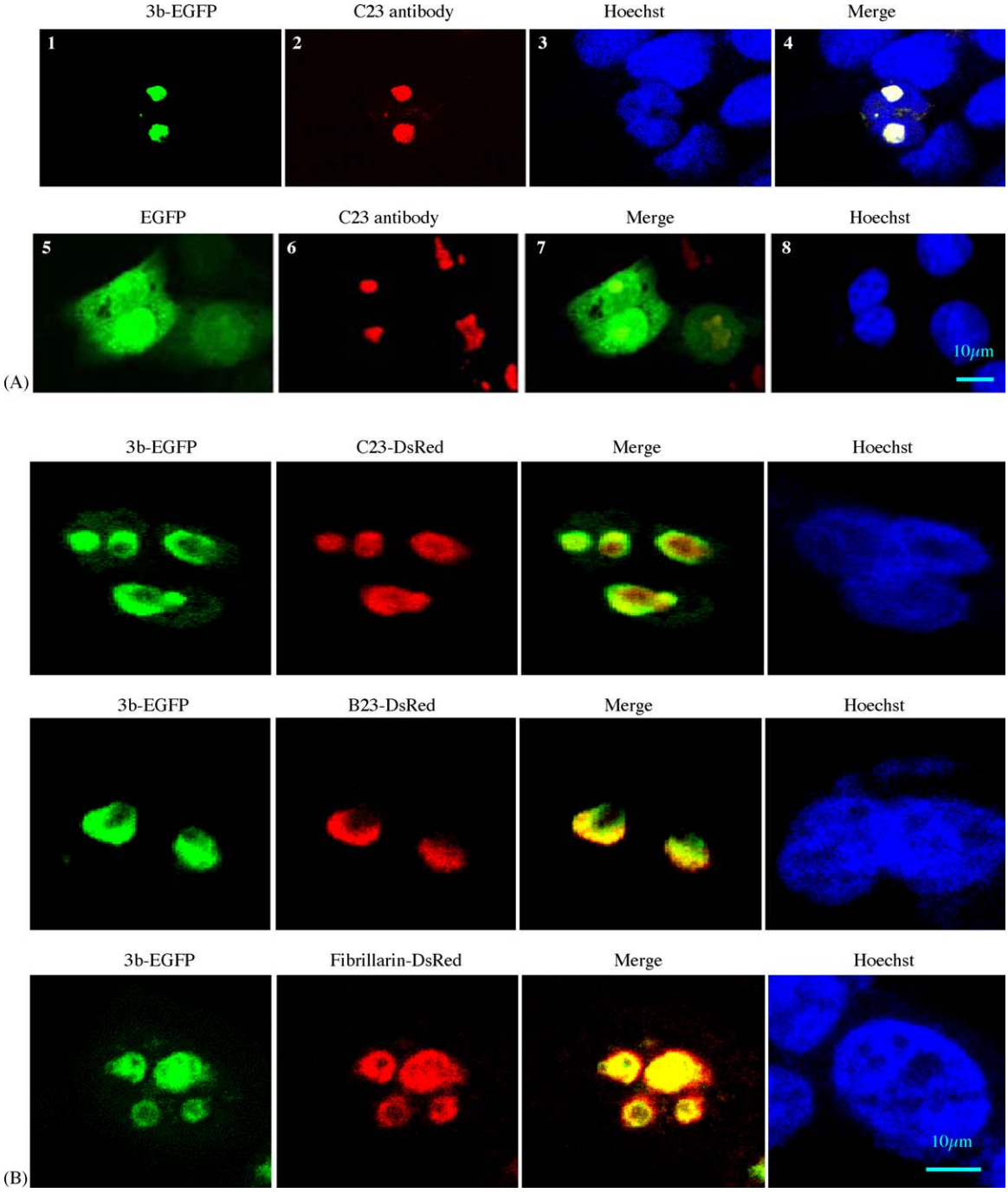

Fig. 2. Subcellular localization of 3b protein. (A) Subcellular localization of 3b protein with C23 antibody. COS-7 cells transfected with p3b-EGFP or pEGFP-N1 plasmid grew for 24 h, then fixed and incubated with a monoclonal antibody against C23, which was detected by TRITC tagged secondary antibody, while the nuclear DNA was stained with Hoechst 33342. p3b-EGFP and pEGFP (green, 1 and 5), fluorescence from C23 antibody (red, 2 and 6) and merge images (4 and 7) were indicated. All four panels of a row have the same field of view. (B) Co-localization of 3b with C23, B23 or fibrillarin protein. The cells co-transfected p3b-EGFP with pC23-DsRed, pB23-DsRed and pfibrillarin-DsRed separately were analyzed by confocal fluorescence microscopy. The merged image were represented regions of overlap between the p3b-EGFP (green) and pC23-DsRed, pB23-DsRed or pfibrillarin-DsRed (red-) image. All four panels of a row have the same field of view.

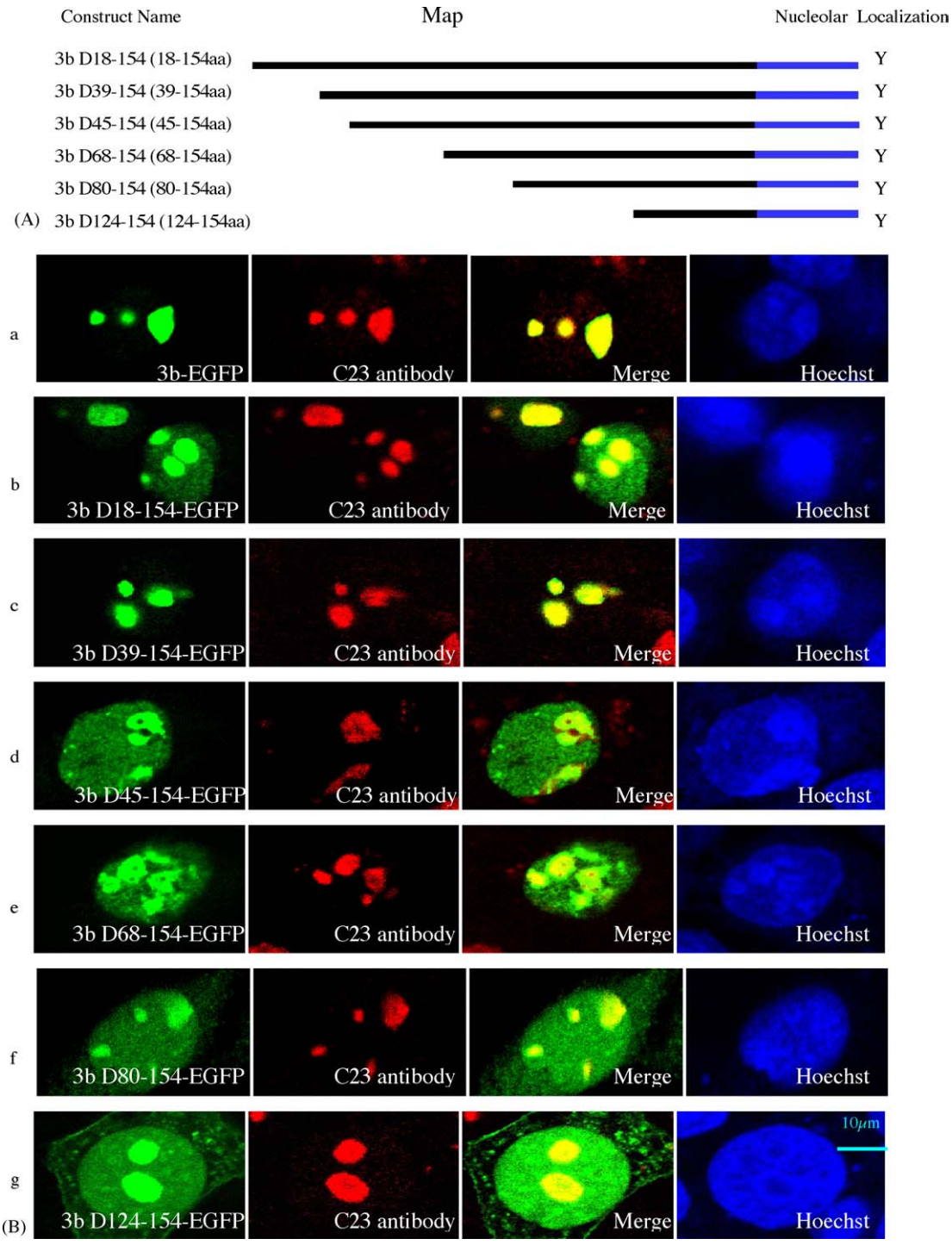

Fig. 3. Co-localization of N-terminal truncated mutants of 3b with C23. (A) DNA constructs of fusion protein. The truncated 3b was cloned into pEGFP-N1 plasmid and expressed as C-terminal fusion protein to EGFP. The amino acid positions for protein 3b were given on the left. The blue line presented the GFP. The statuses of the nucleolar localization were shown on the right, and Y presented yes and N presented no. (B) Co-localization of N-terminal truncated mutants of 3b with C23. At 24 h post-transfection with indicated constructs, COS-7 cells were fixed, permeabilized and incubated with an anti-C23 antibody, which was detected by TRITC antibody, while the nuclear DNA was stained with Hoechst 33342. The samples were examined under confocal fluorescent microscope. The merged image represented region of overlaying the C23 (red-) and p3b-EGFP deletants (green-) image. All four panels of a row have the same field of view.

or C-terminus had little effect on 3b's cellular localization (Fig. 1C). Similar cellular distribution of 3b-EGFP were observed in Vero, COS-7 and A549 cells (Fig. 1D), suggesting that nuclear localization of 3b protein was a conserved attribute.

3.2. Subcellular localization of SARS-CoV 3b protein

Bioinformatics analysis and cellular distribution pattern of 3b both indicated that SARS-CoV 3b might be a nucleolus localization protein. Previous studies showed that some virus proteins, such as coronavirus nucleocapsid protein and HIV rev protein, were localized to the nucleolus through the association with C23, B23 or fibrillarin (Chen et al., 2002; Cheng et al., 2002; Dundr et al., 1995; Yoo et al., 2003). C23/nucleolin, B23/nucleophosmin and fibrillarin all are important nucleolar proteins which localize in nucleolus and involve in ribosomal assembly and biogenesis, rRNA transport and processing RNA transcripts. To confirm 3b's nucleolus localization, we performed co-localizing analysis of p3b-EGFP with C23, B23 and fibrillarin. Indirect immunofluorescence with a monoclonal antibody against C23 was first used to show the nucleolus. As shown in Fig. 2A, 3b-EGFP accumulated mainly in nucleoli in transfected COS-7 cells. Co-transfection of p3b-EGFP with pC23-DsRed, pB23-DsRed and pfibrillarin-DsRed were performed separately and further confirmed that 3b was predominantly localized in the nucleolus in COS-7 cells (Fig. 2B). Using 293 cells, similar results were obtained (data not shown). From the results above, it was deduced that there were nucleolar localization signals (NoLS) in protein 3b, which is able to target exogenous EGFP protein to the nucleolus.

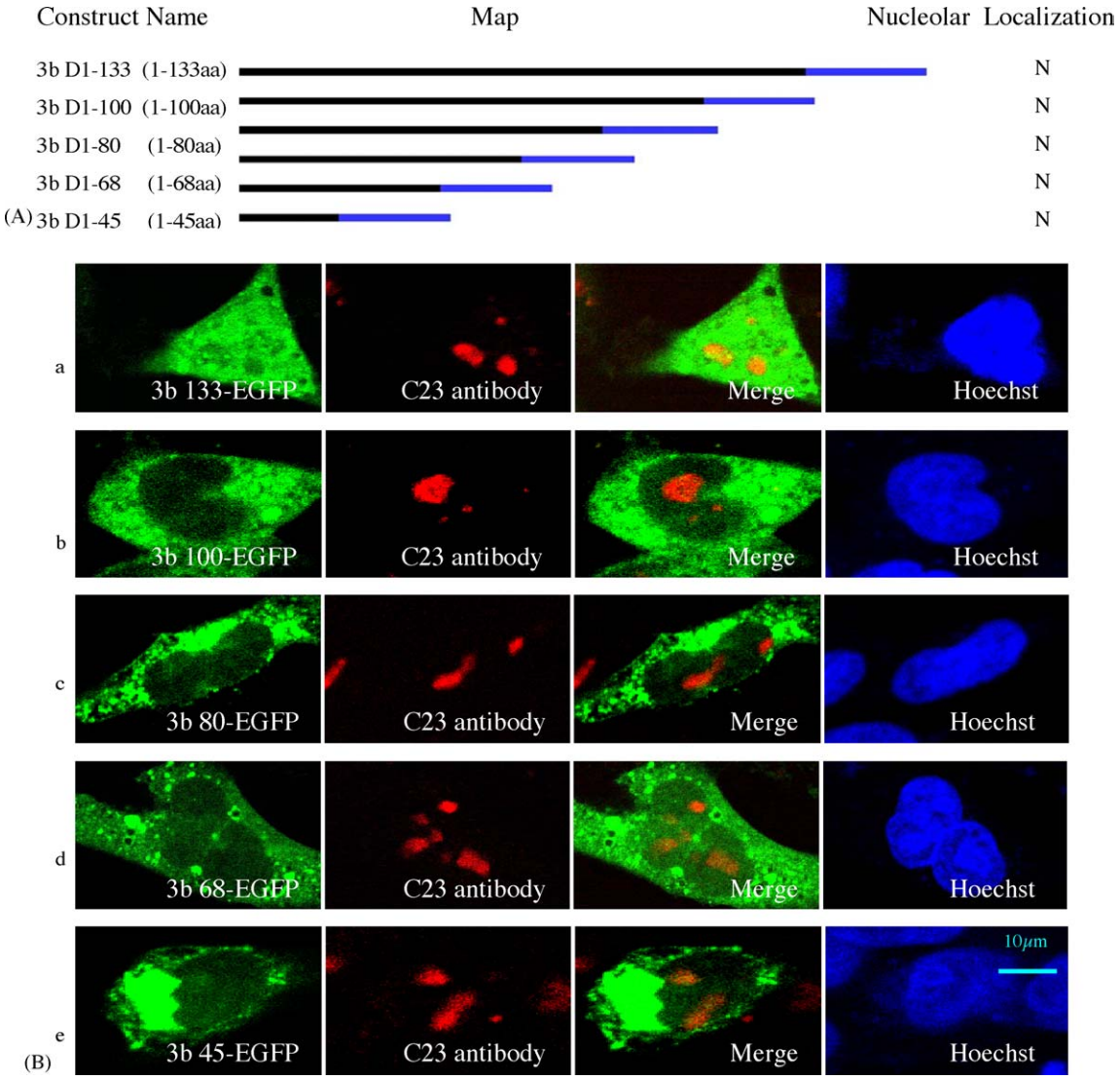

Fig. 4. Co-localization of C-terminal truncated mutants of 3b with C23. (A) DNA constructs of fusion protein. The animo acid positions for protein 3b were given on the left; the statuses of the nucleolar localization were shown on the right. The blue line presented the GFP. (B) Co-localization of C-terminal truncated mutants of p3b-EGFP protein with C23. The merged image represented region of overlaying the C23 (red-) and p3b-EGFP deletants (green-) image. All four panels of a row have the same field of view.

3.3. Determination of the nucleolar localization signals of protein 3b

To define the minimal determinants required for nucleolus targeting, a series of truncated mutants from the N-terminus amino acids of 3b were constructed and their subcellular localizations were examined respectively (Fig. 3A). C23 antibody was used to show the nucleolus as described before. As shown in Fig. 3B, 3b D18-EGFP and D39-EGFP were predominantly localized in nucleolus and seemed to be more accumulation to the nucleolus than that of wild type 3b-EGFP. Further deletions of 3b from 45 to 124 aa (3b D45-EGFP, D68-EGFP, D80-EGFP and D124-EGFP) were all able to efficiently target the EGFP to the nucleolus, but the localization patterns (Fig. 3B) were altered from the characteristic bright fluorescence in nucleolus to some dotted distribution in cytoplasm. These results suggested that C-terminal region from 125 to 154 aa might contain functional NoLS. It was also noted that the nucleolus localization of 3b D18-EGFP and D39-EGFP were more clear than that of wild type one and significantly different from that of 3b D45-EGFP, suggesting the amino acids residues from 40 to 45 may contain another functional NoLS or have an ability in stabilizing the conformation of the nucleolus localization domains.

To determine whether the C-terminal residues are necessary for nucleolar localization, C-terminal deletants of 3b were constructed and their subcellular localizations were examined as before (Fig. 4A). As shown in Fig. 4B, 3b 133-EGFP, which deleted 133 to 154 aa, distributed diffusely throughout both cytoplasm and nucleus. Nucleolus localization of 3b 133-EGFP was not obvious in transfected COS-7 cells. More deletions of 3b from 100 to 45 aa (deletant 3b 100-EGFP, 80-EGFP, 68-EGFP and 45-EGFP) completely abolished the nuclear and nucleolar localization, and only a strong dotted signal in cytoplasm was observed (Fig. 4B, b–e). These results further supported the opinion that the functional NoLS may located at the C-terminus of 3b.

To further determine the functional NoLS in protein 3b, constructs of 3b D134-EGFP and 3b D39-68-EGFP were prepared (Fig. 5A). Both constructs were transiently transfected into COS-7 cells and the co-localization of these fusion proteins with C23 were examined respectively. As shown in Fig. 5B, 3b D134-EGFP construct, containing the predicted NLS, co-localized well with C23 in nucleolus. However, protein 3b D39-68-EGFP that contained no computer-predicted NLS, like pEGFP-N1 vector, distributed diffusely in both cytoplasm and nucleus. Taken together, the nucleolus localization signal of protein 3b may localize in the C-terminal regions from 134 to 154 amino acids, which contains two NLS: NLS1 and bipartite NLS.

To assess the trafficking of protein 3b from cytoplasm to nucleolus, the cellular localization of 3b-EGFP were observed at different times post-transfection. It was revealed that there were no changes in the distribution of p3b-EGFP over time, and nucleolar localization was detected as early as 12 h after transfection (data not shown). Published data showed that transcription inhibitors such as actinomycin D could interrupt the nucleo-cytoplasmic shuttling of some virus protein, such as HTLV Rex protein and HIV Rev protein, and result in the accumulation of virus protein in the cytoplasm (Dundr et al., 1995; Kubota et al., 1996). However, in our experiment, nucleolar localization of protein 3b was not interrupted by the addition of actinomycin D (Fig. 6), suggesting the mechanism of protein 3b on nucleolar local-

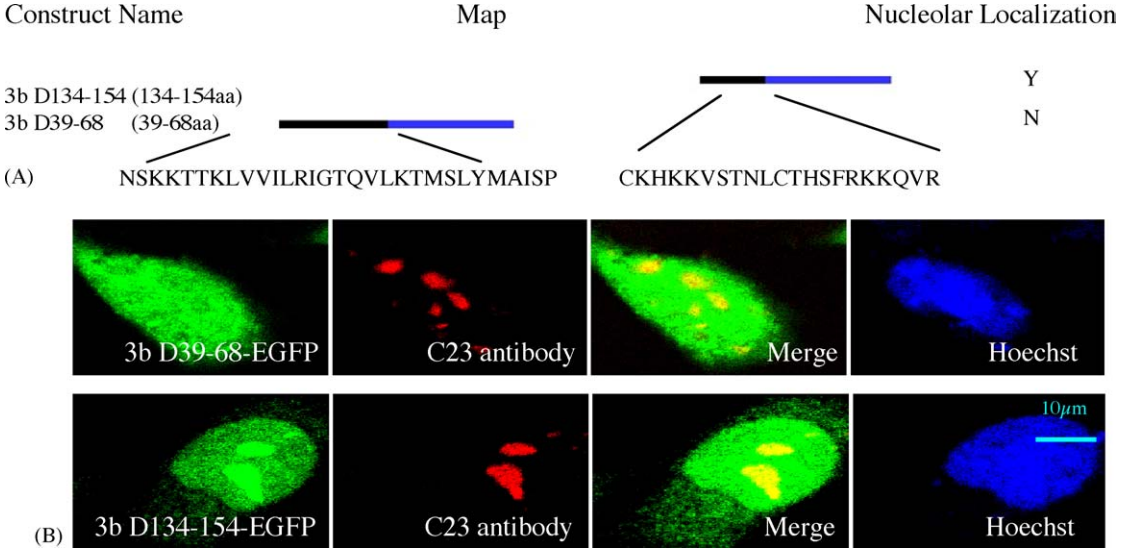

Fig. 5. Identification of the nucleolar localization signal (NoLS) in 3b protein. (A) DNA constructs of fusion protein. The amino acid positions were given on the left, the statuses of the nucleolar localization were shown on the right. The blue line presented the GFP. (B) Determination of the NoLS. The fluorescence allocations were viewed in COS-7 cells transfected with 3b D39-68-EGFP or 3b D134-EGFP fusion plasmids. Expression of 3b D39-68 did not result in the retention of EGFP into nucleolus. However, fluorescence of 3b D134-EGFP was mainly concentrated in the nucleolus. All four panels of a row have the same field of view.

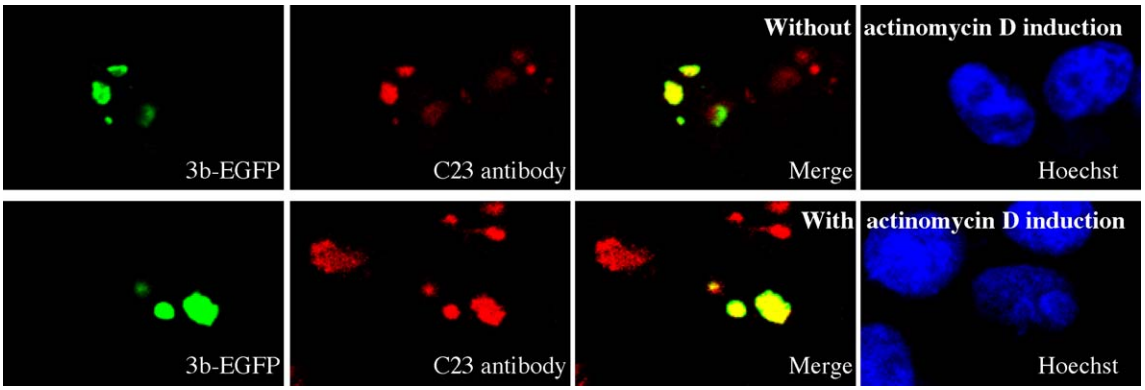

Fig. 6. Effecting of actinomycin D on 3b protein localization. COS-7 cells transfected with 3b-EGFP plasmid were incubated with actinomycin D for 3 h. The fluorescence allocations were viewed as before. All four panels of a row have the same field of view.

ization may be different from that of HTLV Rex and HIV Rev proteins (Strebel, 2003).

The nucleolus is a structure found within nucleus, which plays a key role in ribosome biogenesis (Pederson, 1998). A number of virus proteins have been shown to localize to nucleolus and dysregulated nucleolar functions for virus replication, including human immunodeficiency virus (HIV) type I Rev and Tat (Strebel, 2003), human T-cell leukemia virus (HTLV) Rex (Kubota et al., 1996), and herpes simplex virus (HSV) type 1 gamma (1) 34.5 protein (Cheng et al., 2002). The nucleolus is also the site of Borna disease virus replication and transcription (Pyper et al., 1998). Coronavirus was known to replicate and assembled in the cytoplasm. Using electron microscope, it was observed the virus-like particles in the nucleus of SARS-CoV infected Vero E6 cells at 48 h p.i., and their appearance was similar to that of the nucleocapsids in VMMV (Qinfen et al., 2004). This phenomenon has not been reported in known coronavirus studies. Also it needed to be determined with immune electron microscopy.

Localization to nucleolus is proposed to be a common feature of coronavirus N protein, such as IBV N protein, TGEV N protein and MHV N protein (Hiscox et al., 2001; Wurm et al., 2001). Expression of the TGEV N protein could regulate cell cycle and induce cell cycle delay or arrest, implicating that nucleolus localization of N protein might interfere with host cell translation by disrupting the formation of new ribosome. Recently, it was reported that SARS-CoV N distributed predominantly in cytoplasm and was not found in nucleolus in SARS-CoV infected and transfected Vero-E6 cells (Chang et al., 2004). Interesting, in this article, we observed that SARS-CoV protein 3b was predominately localized to nucleolus in many transfected cells through its potential NoLS. These results inferred that SARS-CoV is different from previously known coronavirus not only in genome but also in the functions of some coronavirus proteins, and these differences may be favorable for the replication and assemblage of SARS-CoV in infected cells (Stavrinides and Guttman, 2004). Till now, the function of SARS-CoV protein 3b in nucleolus is unknown. Much work remains to be done in defining the expression of 3b in SARS-CoV infected cells and elucidating the potential function of 3b in the life cycle of SARS-CoV.

Acknowledgements

We thank Dr. Zhou Tao for technical assistance, Dr. Liu Hongyan, Li Suyan, Yu Zuyin and Li Jianyong for the preparation of plasmids, and Prof. Wei Kang for critical reading of the manuscript. This work was supported by a grant from the Nature Science Foundation of China (30470093).

References

Chang, M.S., Lu, Y.T., Ho, S.T., Wu, C.C., Wei, T.Y., Chen, C.J., Hsu, Y.T., Chu, P.C., Chen, C.H., Chu, J.M., Jan, Y.L., Hung, C.C., Fan, C.C., Yang, Y.C., 2004. Antibody detection of SARS-CoV spike and nucleocapsid protein. Biochem. Biophys. Res. Commun. 314 (4), 931–936.

Chen, H., Wurm, T., Britton, P., Brooks, G., Hiscox, J.A., 2002. Interaction of the coronavirus nucleoprotein with nucleolar antigens and the host cell. J. Virol. 76 (10), 5233–5250.

Cheng, G., Brett, M.E., He, B., 2002. Signals that dictate nuclear, nucleolar, and cytoplasmic shuttling of the gamma(1)34.5 protein of herpes simplex virus type 1. J. Virol. 76 (18), 9434–9445.

Curtis, K.M., Yount, B., Baric, R.S., 2002. Heterologous gene expression from transmissible gastroenteritis virus replicon particles. J. Virol. 76 (3), 1422–1434.

Ding, Y., Wang, H., Shen, H., Li, Z., Geng, J., Han, H., Cai, J., Li, X., Kang, W., Weng, D., Lu, Y., Wu, D., He, L., Yao, K., 2003. The clinical pathology of severe acute respiratory syndrome (SARS): a report from China. J. Pathol. 200 (3), 282–289.

Drosten, C., Gunther, S., Preiser, W., van der Werf, S., Brodt, H.R., Becker, S., Rabenau, H., Panning, M., Kolesnikova, L., Fouchier, R.A., Berger, A., Burguiere, A.M., Cinatl, J., Eickmann, M., Escriou, N., Grywna, K., Kramme, S., Manuguerra, J.C., Muller, S., Rickerts, V., Sturmer, M., Vieth, S., Klenk, H.D., Osterhaus, A.D., Schmitz, H., Doerr, H.W., 2003. Identification of a novel coronavirus in patients with severe acute respiratory syndrome. N. Engl. J. Med. 348 (20), 1967–1976.

Dundr, M., Leno, G.H., Hammarskjold, M.L., Rekosh, D., Helga-Maria, C., Olson, M.O., 1995. The roles of nucleolar structure and function in the subcellular location of the HIV-1 Rev protein. J. Cell. Sci. 108 (8), 2811–2823.

Fan, K., Wei, P., Feng, Q., Chen, S., Huang, C., Ma, L., Lai, B., Pei, J., Liu, Y., Chen, J., Lai, L., 2004. Biosynthesis, purification and substrate specificity of SARS coronavirus 3C-like proteinase. J. Biol. Chem. 279 (3), 1637–1642.

Fouchier, R.A., Kuiken, T., Schutten, M., van Amerongen, G., van Doornum, G.J., van den Hoogen, B.G., Peiris, M., Lim, W., Stohr, K., Osterhaus, A.D., 2003. Aetiology: Koch's postulates fulfilled for SARS virus. Nature 423 (6937), 240.

Haijema, B.J., Volders, H., Rottier, P.J., 2004. Live, attenuated coronavirus vaccines through the directed deletion of group-specific genes provide protection against feline infectious peritonitis. J. Virol. 78 (8), 3863–3871.

Herrewegh, A.A., Vennema, H., Horzinek, M.C., Rottier, P.J., de Groot, R.J., 1995. The molecular genetics of feline coronaviruses: comparative sequence analysis of the ORF7a/7b transcription unit of different biotypes. Virology 212 (2), 622–631.

Hiscox, J.A., Wurm, T., Wilson, L., Britton, P., Cavanagh, D., Brooks, G., 2001. The coronavirus infectious bronchitis virus nucleoprotein localizes to the nucleolus. J. Virol. 75 (1), 506–512.

Hofmann, H.J., Hadge, D., 1987. On the theoretical prediction of protein antigenic determinants from amino acid sequences. Biomed. Biochim. Acta 46 (11), 855–866.

Ksiazek, T.G., Erdman, D., Goldsmith, C.S., Zaki, S.R., Peret, T., Emery, S., Tong, S., Urbani, C., Comer, J.A., Lim, W., Rollin, P.E., Dowell, S.F., Ling, A.E., Humphrey, C.D., Shieh, W.J., Guarner, J., Paddock, C.D., Rota, P., Fields, B., DeRisi, J., Yang, J.Y., Cox, N., Hughes, J.M., LeDuc, J.W., Bellini, W.J., Anderson, L.J., 2003. A novel coronavirus associated with severe acute respiratory syndrome. N. Engl. J. Med. 348 (20), 1953–1966.

Kubota, S., Hatanaka, M., Pomerantz, R.J., 1996. Nucleo-cytoplasmic redistribution of the HTLV-I Rex protein: alterations by coexpression of the HTLV-I p21x protein. Virology 220 (2), 502–507.

Lang, Z., Zhang, L., Zhang, S., Meng, X., Li, J., Song, C., Sun, L., Zhou, Y., 2003. Pathological study on severe acute respiratory syndrome. Chin. Med. J. (Engl.) 116 (7), 976–980.

Le, S.Y., Sonenberg, N., Maizel Jr., J.V., 1994. Distinct structural elements and internal entry of ribosomes in mRNA3 encoded by infectious bronchitis virus. Virology 198 (1), 405–411.

Lee, N., Hui, D., Wu, A., Chan, P., Cameron, P., Joynt, G.M., Ahuja, A., Yung, M.Y., Leung, C.B., To, K.F., Lui, S.F., Szeto, C.C., Chung, S., Sung, J.J., 2003. A major outbreak of severe acute respiratory syndrome in Hong Kong. N. Engl. J. Med. 348 (20), 1986–1994.

Liu, D.X., Cavanagh, D., Green, P., Inglis, S.C., 1991. A polycistronic mRNA specified by the coronavirus infectious bronchitis virus. Virology 184 (2), 531–544.

Liu, D.X., Inglis, S.C., 1992. Internal entry of ribosomes on a tricistronic mRNA encoded by infectious bronchitis virus. J. Virol. 66 (10), 6143–6154.

Marra, M.A., Jones, S.J., Astell, C.R., Holt, R.A., Brooks-Wilson, A., Butterfield, Y.S., Khattra, J., Asano, J.K., Barber, S.A., Chan, S.Y., Cloutier, A., Coughlin, S.M., Freeman, D., Girn, N., Griffith, O.L., Leach, S.R., Mayo, M., McDonald, H., Montgomery, S.B., Pandoh, P.K., Petrescu, A.S., Robertson, A.G., Schein, J.E., Siddiqui, A., Smailus, D.E., Stott, J.M., Yang, G.S., Plummer, F., Andonov, A., Artsob, H., Bastien, N., Bernard, K., Booth, T.F., Bowness, D., Czub, M., Drebot, M., Fernando, L., Flick, R., Garbutt, M., Gray, M., Grolla, A., Jones, S., Feldmann, H., Meyers, A., Kabani, A., Li, Y., Normand, S., Stroher, U., Tipples, G.A., Tyler, S., Vogrig, R., Ward, D., Watson, B., Brunham, R.C., Krajden, M., Petric, M., Skowronski, D.M., Upton, C., Roper, R.L., 2003. The Genome sequence of the SARS-associated coronavirus. Science 300 (5624), 1399–1404.

Nakai, K., Kanehisa, M., 1992. A knowledge base of predicting protein localization sites in eukatyotic cells. Genomics 14 (4), 897–911.

Nicholls, J.M., Poon, L.L., Lee, K.C., Ng, W.F., Lai, S.T., Leung, C.Y., Chu, C.M., Hui, P.K., Mak, K.L., Lim, W., Yan, K.W., Chan, K.H., Tsang, N.C., Guan, Y., Yuen, K.Y., Peiris, J.S., 2003. Lung pathology of fatal severe acute respiratory syndrome. Lancet 361 (9371), 1773–1778.

Paul, P.S., Vaughn, E.M., Halbur, P.G., 1997. Pathogenicity and sequence analysis studies suggest potential role of gene 3 in virulence of swine enteric and respiratory coronaviruses. Adv. Exp. Med. Biol. 412, 317–321.

Pederson, T., 1998. The plurifunctional nucleolus. Nucleic Acids Res. 26 (17), 3871–3876.

Peiris, J.S., Lai, S.T., Poon, L.L., Guan, Y., Yam, L.Y., Lim, W., Nicholls, J., Yee, W.K., Yan, W.W., Cheung, M.T., Cheng, V.C., Chan, K.H., Tsang, D.N., Yung, R.W., Ng, T.K., Yuen, K.Y., 2003. Coronavirus as a possible cause of severe acute respiratory syndrome. Lancet 361 (9366), 1319–1325.

Pyper, J.M., Clements, J.E., Zink, M.C., 1998. The nucleolus is the site of Borna disease virus RNA transcription and replication. J. Virol. 72 (9), 7697–7702.

Qinfen, Z., Jinming, C., Xiaojun, H., Huanying, Z., Jicheng, H., Ling, F., Kunpeng, L., Jingqiang, Z., 2004. The life cycle of SARS coronavirus in Vero E6 cells. J. Med. Virol. 73 (3), 332–337.

Rota, P.A., Oberste, M.S., Monroe, S.S., Nix, W.A., Campagnoli, R., Icenogle, J.P., Penaranda, S., Bankamp, B., Maher, K., Chen, M.H., Tong, S., Tamin, A., Lowe, L., Frace, M., DeRisi, J.L., Chen, Q., Wang, D., Erdman, D.D., Peret, T.C., Burns, C., Ksiazek, T.G., Rollin, P.E., Sanchez, A., Liffick, S., Holloway, B., Limor, J., McCaustland, K., Olsen-Rasmussen, M., Fouchier, R., Gunther, S., Osterhaus, A.D., Drosten, C., Pallansch, M.A., Anderson, L.J., Bellini, W.J., 2003. Characterization of a novel coronavirus associated with severe acuterespiratorysyndrome. Science 300 (5624), 1394–1399.

Shen, S., Wen, Z.L., Liu, D.X., 2003. Emergence of a coronavirus infectious bronchitis virus mutant with a truncated 3b gene: functional characterization of the 3b protein in pathogenesis and replication. Virology 311 (1), 16–27.

Stavrinides, J., Guttman, D.S., 2004. Mosaic evolution of the severe acute respiratory syndrome coronavirus. J. Virol. 78 (1), 76–82.

Strebel, K., 2003. Virus–host interactions: role of HIV proteins Vif, Tat, and Rev. AIDS 17 (Suppl. 4), S25–S34.

Thiel, V., Ivanov, K.A., Putics, A., Hertzig, T., Schelle, B., Bayer, S., Weissbrich, B., Snijder, E.J., Rabenau, H., Doerr, H.W., Gorbalenya, A.E., Ziebuhr, J., 2003. Mechanisms and enzymes involved in SARS coronavirus genome expression. J. Gen. Virol. 84 (9), 2305–2315.

Tsang, K.W., Ho, P.L., Ooi, G.C., Yee, W.K., Wang, T., Chan-Yeung, M., Lam, W.K., Seto, W.H., Yam, L.Y., Cheung, T.M., Wong, P.C., Lam, B., Ip, M.S., Chan, J., Yuen, K.Y., Lai, K.N., 2003. A cluster of cases of severe acute respiratory syndrome in Hong Kong. N. Engl. J. Med. 348 (20), 1977–1985.

WHO, 2003. A multicentre collaboration to investigate the cause of severe acute respiratory syndrome. Lancet. 361 (9370), 1730–1733.

Wurm, T., Chen, H., Hodgson, T., Britton, P., Brooks, G., Hiscox, J.A., 2001. Localization to the nucleolus is a common feature of coronavirus nucleoproteins, and the protein may disrupt host cell division. J. Virol. 75 (19), 9345–9356.

Yoo, D., Wootton, S.K., Li, G., Song, C., Rowland, R.R., 2003. Colocalization and interaction of the porcine arterivirus nucleocapsid protein with the small nucleolar RNA-associated protein fibrillarin. J. Virol. 77 (22), 12173–12183.

Yuan, X., Cong, Y., Hao, J., Shan, Y., Zhao, Z., Wang, S., Chen, J., 2004. Regulation of LIP level and ROS formation through interaction of H-ferritin with G-CSF receptor. J. Mol. Biol. 339 (1), 131–144.

Yuan, X., Li, J., Shan, Y., Yang, Z., Zhao, Z., Chen, B., Yao, Z., Dong, B., Wang, S., Chen, J., Cong, Y., 2005. Subcellular localization and membrane association of SARS-CoV 3a protein. Virus. Res. 109 (2), 191–202.